

DESIGNING MAGNETIC NANOPARTICLES FOR PROTEIN SEPARATION – A COMPARATIVE STUDY BETWEEN FLAME SPRAY PYROLYSIS AND SOL-GEL SYNTHESIS

*Cordelia Selomulya*¹, *Li Dan*², *Wey Yang Teoh*², *Robert Woodward*³, and *Rose Amal*²

1 Department of Chemical Engineering, Clayton Campus, Monash University, Melbourne VIC 3800, AUSTRALIA

2 ARC Centre for Functional Nanomaterials, The University of New South Wales, Sydney NSW 2032, AUSTRALIA

3 School of Physics, The University of Western Australia, Crawley WA 6009, AUSTRALIA
cordelia.selomulya@eng.monash.edu.au

The application of magnetic particles in the field of biological and biomedical science can be traced back to the 1970s where micron-sized particles were used as support material for enzyme immobilization [1] and bioaffinity adsorbents [2]. Success in synthesizing nano-sized magnetic particles has empowered a wider range of exciting bio-applications, including magnetic resonance imaging (MRI) [3], bioseparation [4], and drug delivery [5]. The ideal properties of magnetic nanostructures (depending on the specific application) would be uniform size, large surface area, fast adsorption kinetics, biocompatibility, and superparamagnetism with high magnetic strength. Often, an additional inorganic or polymeric coating layer is necessary to avoid the aggregation of magnetic cores and to improve the functionality or biocompatibility of the nanostructures. Despite ongoing research efforts in the search for reliable synthesis routes allowing the control of these properties, wet chemistry-based methods such as micro-emulsion, sonochemical, reverse micelles, and sol-gel techniques are inherently limited in scalability. On the other hand, Flame Spray Pyrolysis (FSP) has been demonstrated as a rapid, scalable and waste-free production technique with a production rate 600 g/h of nanoparticles on a pilot scale [6]. The use of FSP-synthesized magnetic particles with tailored properties for specific bio-related applications thus has great potentials.

In this study, Flame Spray Pyrolysis (FSP) was used to synthesize maghemite (γ -Fe₂O₃) nanoparticles of BET-equivalent diameter (d_{BET}) of 5nm, 13nm, and 20nm. Composite nanostructures of SiO₂/ γ -Fe₂O₃ with different Fe:Si molar ratios were also produced using either a one-step FSP method or by sol-gel coating of silica onto the FSP-produced 13nm γ -Fe₂O₃ core [Figure 1]. The physical, chemical and magnetic properties of the γ -Fe₂O₃ and SiO₂/ γ -Fe₂O₃ nanostructures were characterised and compared. The nanostructures were predominantly superparamagnetic at room temperature, with saturation magnetism decreasing with γ -Fe₂O₃ size and the thickness of silica coating [Figure 2]. To observe the potential use of these particles for protein separation, adsorption and desorption of bovine serum albumin (BSA) onto γ -Fe₂O₃ and SiO₂/ γ -Fe₂O₃ particles were studied in phosphate and formate buffers. Highest BSA binding capacity of 373±20mg/g with a dissociation constant of 0.016gL⁻¹ was obtained for FSP 5nm γ -Fe₂O₃ in 10mM formate buffer [Figure 3(a)]. The binding capacity is influenced predominantly by suspension chemistry that altered the electrostatic interaction of particles surfaces and BSA, and by the particle surface properties affecting the hydrophobic interaction with BSA and the number of binding sites available as a function of specific surface area. BSA desorption was best achieved by shifting the pH of suspension from 5.3 to 9 using K₂HPO₄ [Figure 3(b)]. The substantial affinity of BSA towards the particles surface, coupled with mild desorption conditions and easy recovery under external magnetic field render these particles ideal for protein separation purposes. Furthermore, the silica layer could be functionalised for specific ligands attachment via the well established silane coupling chemistry to introduce selectivity. The synthesized particles are promising nanomaterials for efficient bioseparation.

References:

1. Robinson, P. J., Dunnill, P. and Lilly, M.D., *Biotechnology and Bioengineering*, **15** (1973) 603-606.
2. Dunnill, P. and Lilly, M.D., *Biotechnology and Bioengineering*, **16** (1974) 987-990.
3. Bomati-Miguel, O., Morales, M.P., Tartaj, P., Ruiz-Cabello, J., Bonville, P., Santos, M., Zhao, X. and Veintemillas-Verdaguer, S., *Biomaterials*, **26** (2005) 5695-5703.
4. Bucak S., Jones D. A., Laibinis P.E. and Hatton T.A., *Biotechnology Progress*, **19** (2003) 477-484.
5. Yu, S. and Chow, G.M, *Journal of Materials Chemistry*, **14** (2004) 2781-2786.
6. Mueller, R., Jossen, R., Pratsinis, S. E., Watson, M. and Akhtar, M. K. *Journal of American Ceramics Society*, **87**(2) (2004) 197-202.

Figures:

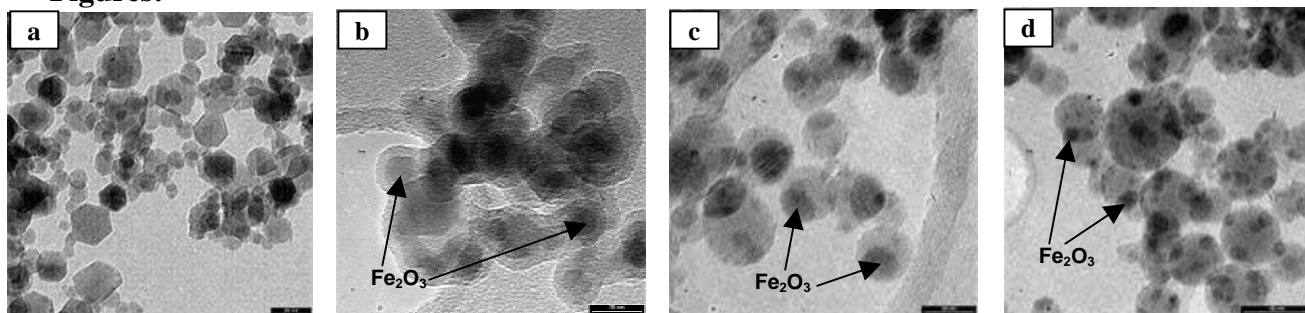


Figure 1 – FSP-synthesized $\gamma\text{-Fe}_2\text{O}_3$ of (a) $d_{BET} = 20\text{ nm}$; (b) sol-gel coated SiO_2 on 13 nm FSP $\gamma\text{-Fe}_2\text{O}_3$ with $\text{Fe}:\text{Si} = 1:1$; (c) one-step FSP-synthesized $\text{SiO}_2/\gamma\text{-Fe}_2\text{O}_3$ with $\text{Fe}:\text{Si} = 1:2$ and (d) $\text{Fe}:\text{Si} = 1:5$

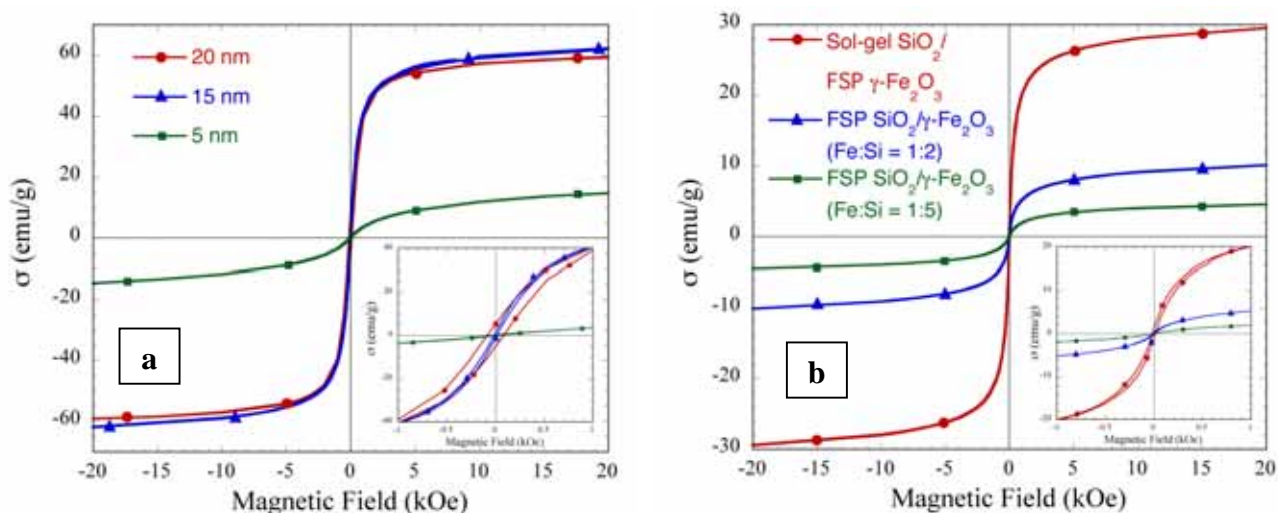


Figure 2 – Hysteresis loops at 300K for (a) d_{BET} 5 nm, 13 nm, and 20 nm $\gamma\text{-Fe}_2\text{O}_3$; (b) $\text{SiO}_2/\gamma\text{-Fe}_2\text{O}_3$ particles

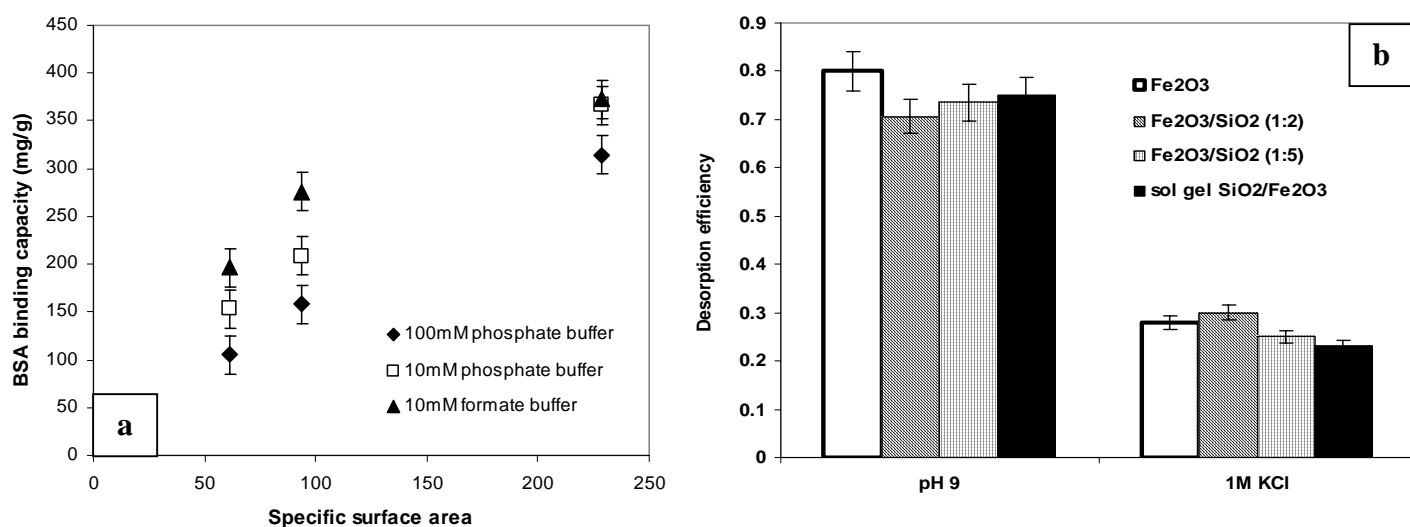


Figure 3 – (a) BSA binding capacity at $2.5 \pm 0.1\text{ g/L}$ particle loading and room temperature after 3hr adsorption as a function of specific surface area; (b) % BSA desorbed in phosphate buffer